**Journal of NeuroVirology,** 14: 239–251, 2008
ISSN: 1355-0284 print / 1538-2443 online
DOI: 10.1080/13550280802093919

informa
healthcare

# Down-regulation of Jab1, HIF-1$\alpha$, and VEGF by Moloney murine leukemia virus-*ts1* infection: A possible cause of neurodegeneration

Gina F Lungu,[1] George Stoica,[1] and Paul KY Wong[2]

[1]*Department of Pathobiology, College of Veterinary Medicine, Texas A&M University, College Station Texas, USA; and* [2]*Department of Carcinogenesis, The University of Texas M.D. Anderson Cancer Center Science Park–Research Division, Smithville, Texas, USA*

**Moloney murine leukemia virus–temperature sensitive (MoMuLV-*ts*1)-mediated neuronal death is a result of both loss of glial support and release of cytokines and neurotoxins from *ts*1-infected glial cells. Here the authors propose vascular endothelial growth factor (VEGF) down-regulation as another contributory factor in neuronal degeneration induced by *ts1* infection. To determine how *ts*1 affects VEGF expression in *ts*1-infected brain, the authors examined the expression of several proteins that are important in regulating the expression of VEGF. The authors found significant decreases in Jun-activating domain-binding protein 1 (Jab1), hypoxia-inducible factor (HIF)-1$\alpha$, and VEGF levels and increases in p53 protein levels in *ts1*-infected brains compared to noninfected control brains. The authors suggest that a decrease Jab1 expression in *ts*1 infection leads to accumulation of p53, which binds to HIF-1$\alpha$ to accelerate its degradation. A rapid degradation of HIF-1$\alpha$ leads to decreased VEGF production and secretion. Considering that endothelial cells are the most conspicuous in virus replication and production in *ts*1 infection, but are not killed by the infection, the authors examined the expression of these proteins using infected and noninfected mouse cerebrovascular endothelial (CVE) cells. The *ts1*-infected CVE cells showed decreased Jab1, HIF-1$\alpha$, and VEGF mRNA and protein levels and increased p53 protein levels compared with noninfected cells, consistent with the results found *in vivo*. These results confirm that *ts*1 infection results in insufficient secretion of VEGF from endothelial cells and may result in decreased neuroprotection. This study suggested that *ts*1-mediated neuropathology in mice may result from changes in expression and activity of Jab1, p53, and HIF-1$\alpha$, with a final target on VEGF expression and neuronal degeneration.** *Journal of NeuroVirology* (2008) **14,** 239–251.

**Keywords:** CVE cells; HIF-1$\alpha$; Jab1; MoMuLV-*ts*1; neuronal degeneration; p53; VEGF

## Introduction

The pathogenesis of a progressive murine spongiform encephalomyelopathy induced by a neuropathogenic mutant of Moloney murine leukemia virus–TB, MoMuLV-*ts*1, has been investigated for many years in our laboratory. MoMuLV-*ts*1 is a type C retrovirus that induces T-cell lymphomas in susceptible strains of mice at 6 to 8 months of age (Yuen and Szurek, 1989). A single point mutation in the envelope gene of its temperature-sensitive mutant *ts*1 confers upon the virus the ability to deplete T cells and motor neurons in mice by 6 weeks of age (Wong *et al*, 1989; Szurek *et al*, 1990; Wong *et al*, 1991). MoMuLV-*ts*1 possesses the ability to induce bilateral hind-limb paralysis and immunodeficiency in infected mice (Wong *et al*, 1985), which become evident between 25 and 30 days post inoculation (d.p.i.). The disease is also associated with the development of thymic and

Address correspondence to P. K. Y. Wong, PhD, Department of Carcinogenesis, The University of Texas M.D. Anderson Cancer Center, Science Park–Research Division, 1808 Park Road 1C, Smithville, TX 78957, USA. E-mail: pkwong@mdanderson.org

This work was supported by National Institutes of Health grants 5R01 MH071583 18 and 2R01 NS043984 05 A1 awarded to P. K. Y. Wong. The authors are grateful to Dr. Jane Welsh for providing the BALB/c mice CVE cell line. They thank Xueyi Xie for technical assistance.



Received 16 January 2008; revised 15 February 2008; accepted 28 March 2008.

splenic atrophy (Prasad *et al*, 1989). Previous studies showed that infection of the central nervous system (CNS) with *ts*1 causes a progressive neurodegenerative disease. The CNS microscopic lesions of *ts*1-infected mice consist of vacuolar degeneration of motor neurons and spongy changes of white matter in the brainstem, cerebellum, and spinal cord (Stoica *et al*, 1993; Stoica *et al*, 2000). Our previous results (Stoica *et al*, 1993) demonstrated that productive *ts*1 infection in the brain occurs in endothelial cells. Astrocytes, ependymal cells, microglia, oligodendrocytes are also infected, but not neurons, inferring an indirect mechanism in *ts*1-mediatd neuronal degeneration. Taken together, the disease pathogenesis is non-cell-autonomous, with toxicity derived from glia as a primary contributor driving disease initiation and progression.

Among the murine retroviruses, *ts*1 is similar to human immunodeficiency virus (HIV) in its use of CD4+ cells for infection, its secondary neurocytopathic effect, its continuous viremia with free virus in the circulation and depletion of CD4+ cells. These and other similarities have led to its use as an animal model for HIV (Clark *et al*, 2001).

Virus infections affect cell division by interfering with cell cycle regulation or altering cellular gene expression (Kim *et al*, 2002). Previous studies demonstrated that p53, a transcriptional factor important in regulation of growth arrest, apoptosis, and differentiation, plays a critical role in the cellular response to environmental stress, and is increased in the brainstem of *ts*1-infected mice and in *ts*1-infected C1 astrocytes (Kim *et al*, 2002). One of the proteins responsible for p53 cytoplasmic localization, which subsequent leads to the degradation of p53, is Jun-activating domain-binding protein 1 (Jab1).

Jab1, also known as COP9 signalosome subunit 5 (CSN5), is a component of the COP9 signalosome regulatory complex (CSN). Jab1 was first identified as a transcriptional activator of c-Jun and Jun D, stabilizing the formation of the activator protein (AP)-1 complex, a transcription factor (Lee *et al*, 2006). It was demonstrated that Jab1 alone was able to induce cytoplasmic translocation and degradation of nuclear p53 (Oh *et al*, 2006). Jab1 knockout mice had higher p53 levels, suggesting a role of Jab1 in p53 homeostasis (Tomoda *et al*, 2004). In fact, it was suggested that levels of both nuclear and cytoplasmic p53 are actually controlled by Jab1 or CSN complexes (Bech-Otschir *et al*, 2001; Oh *et al*, 2006). Jab1 may be involved in the onset of neurodegenerative diseases caused by endoplasmic reticulum (ER) dysfunction. Jab1 was shown to bind to inositol-requiring enzyme (IRE)1$\alpha$, one of the ER stress transducers, during resting conditions. Mild ER stress enhanced this reaction, whereas strong ER stress diminished it. Thus, Jab1 might regulate the choice between the unfolded protein response (UPR) and apoptosis by association with or dissociation from IRE1 (Oono *et al*, 2004).

One interesting function of Jab1 is its ability to promote oncogenesis by stabilizing hypoxia-inducible factor 1alpha (HIF-1$\alpha$), a transcription factor that controls expression of a number of genes under low cellular oxygen concentration (Lee *et al*, 2006). HIF-1$\alpha$ is the major transcription factor responsible for induction of vascular endothelial growth factor (VEGF) production and secretion. VEGF secreted by glial cells or/and endothelial cells is neuroprotective and significantly contributes to neuronal protection especially in hypoxic conditions. Previous reports demonstrated that knockout mice, in which hypoxic regulation of VEGF was impaired, exhibited signs of motor neuron degeneration, similar to those seen in humans with amyotrophic lateral sclerosis (Oosthuyse *et al*, 2001). VEGF also affects neuronal death after acute spinal cord or cerebral ischemia, and has been implicated in other neurological disorders such as ischemic neuropathy, nerve degeneration, Parkinson's disease, Alzheimer's disease, and multiple sclerosis (Storkebum *et al*, 2004). Thus, a loss of function or rapid degradation of HIF-1$\alpha$ could alter the ability of glial or endothelial cells to provide neurotrophic support to neurons, leading to neuronal loss.

Previous studies suggested that HIF-1$\alpha$ becomes unstable when bound to p53 (Ravi *et al*, 2000) and Jab1 protein directly interferes with the HIF-1$\alpha$–p53 complex and leads to stabilization of the HIF-1$\alpha$ protein during hypoxia (Bae *et al*, 2002). Although some studies suggested that p53 interacts with HIF-1$\alpha$ and suppresses its function (Ravi *et al*, 2000), recent work reported that p53 does not alter HIF-1$\alpha$ protein abundance or function during hypoxia (Rempe *et al*, 2007), which suggests that influence of p53 on HIF-1$\alpha$ protein abundance and function is probably a cell type–specific phenomenon.

The aim of this study was to elucidate the contribution of Jab1, p53, and HIF-1$\alpha$ proteins to VEGF expression and neuronal degeneration in MoMuLV-*ts*1–infected CNS of FVB/N mice. In both *ts*1-infected mouse brain and *ts*1-infected mouse cerebrovascular endothelial (CVE) cells, a decrease in Jab1, HIF-1$\alpha$, VEGF, and an increase in p53 expression, was observed. Our studies suggest that down-regulation of Jab1 might be one of the factors responsible for the p53 increase, which leads to a rapid degradation of HIF-1$\alpha$ and a reduction in VEGF levels in *ts*1 infection. Reduced VEGF levels can lead to neuronal cell death due to loss of neuroprotection, especially in conditions of severe hypoxia caused by *ts*1 infection. Thus, we highlight the loss of VEGF-mediated neuroprotection in retroviral infection-induced neuronal cell degeneration and death *in vivo*.

## Results

### *Decreased levels of Jab1, HIF-1α, and VEGF in the brain of ts1-infected mice*

Using Western blot (WB) analysis, we assessed the expression of Jab1, HIF-1$\alpha$, and VEGF in whole-brain

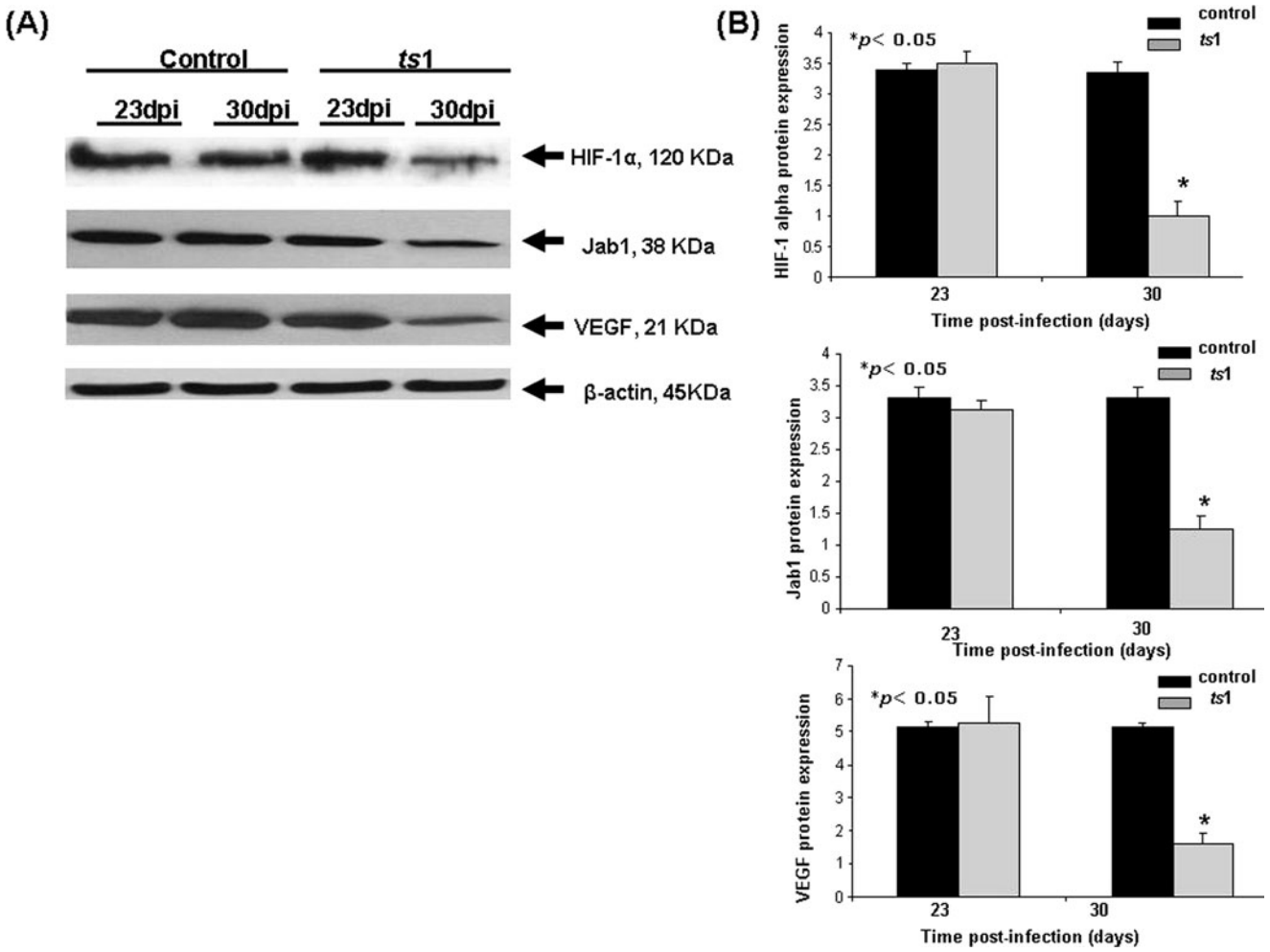


**Figure 1** Expression of Jab1, HIF-1$\alpha$, and VEGF in brains of controls and *ts*1-infected mice. (**A**) Western blots showing levels of Jab1, HIF-1$\alpha$, and VEGF proteins in whole brain of controls versus *ts*1-infected mice at 23 and 30 days post infection (d.p.i.). At 23 and 30 d.p.i., tissues homogenates were prepared from whole brain of control and *ts*1-infected mice and subjected to immunobloting analysis. $\beta$-actin served as a loading control. (**B**) Densitometric analysis of Jab1, HIF-1$\alpha$, and VEGF protein levels in the whole brain of *ts*1-infected versus control mice. Amounts of Jab1, HIF-1$\alpha$, and VEGF proteins in the whole brains of *ts*1-infected mice were significantly decreased at 30 d.p.i., compared to those of the brains of control mice. The results represent the mean $\pm$ standard deviation for three independent experiments. Asterisks indicate statistically significant differences ($^* p < .05$).

homogenates from control and *ts1*-infected mice. As shown in Figure 1A and B, there is a decrease in Jab1, HIF-1$\alpha$, and VEGF protein expression in *ts1*-infected mouse brain at 30 days post infection (d.p.i.), but no significant changes in their levels at 23 d.p.i. where pathology is less severe.

In addition to WB analysis, we performed immunohistochemistry (IHC) to localize these proteins in control and *ts1*-infected brains. Although we analyzed the expression of these proteins throughout the brain, we present here data from brainstem of control and *ts1*-infected mice because this is one of the CNS regions consistently showing spongiform changes. In the brainstem of control mice, many neurons and glial cells showed intense cytoplasmic and nuclear labeling for Jab1 (Figure 2A to C), with less Jab1 immunolabeling in *ts1*-infected brainstem (Figure 2D to F). Jab1 protein expression was also very intense in endothelial cells lining blood vessels of control mice (Figure 2C) and virtually absent in endothelial cells lining blood vessels of *ts*1-infected mice (Figure 2F). The expression of HIF-1$\alpha$ was intense in both cytoplasm and nucleus of neurons and glial cells in control mice brainstem (Figure 3A and B), but weaker in the neurons and glial cells in *ts1*-infected brainstem (Figure 3C and D). The expression pattern of VEGF was very similar to the expression of Jab1 and HIF-1$\alpha$ with intense label of neurons and glial cells in brainstem (Figure 4A and B) of control mice and decreased labeling in *ts1*-infected brainstem neurons (Figure 4C and D). Taken together, the results from IHC demonstrate that there is a reduction of Jab1, HIF-1$\alpha$, and VEGF protein in *ts1*-infected mice brainstem compared with control mice brainstem.

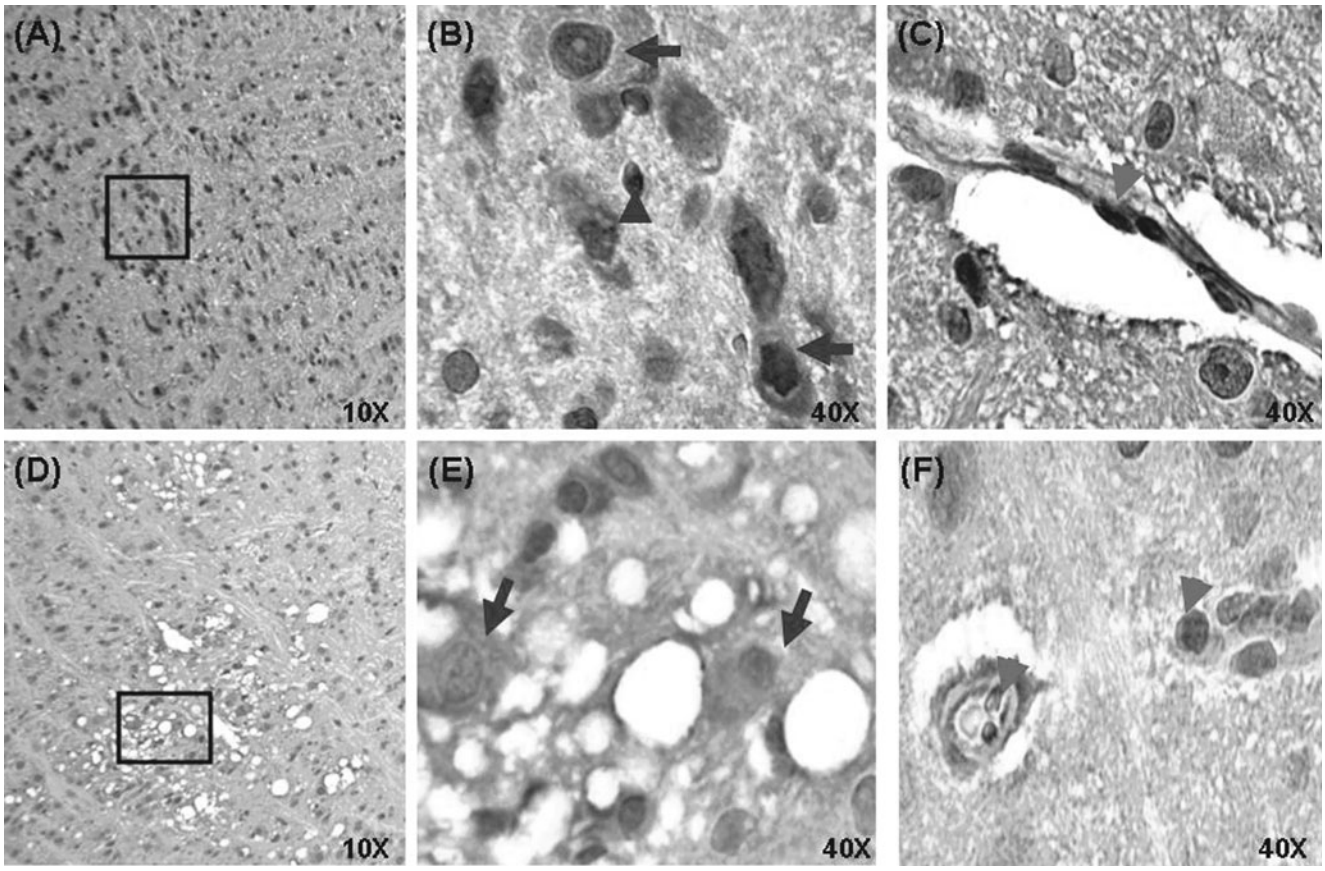


**Figure 2** Expression of Jab1 in brainstem of control versus *ts*1-infected mice. (**A**) Marked Jab1 immunoreactivity in the cytoplasm and nucleus of neurons and glial cells in the brainstem of control mice (at 30 d.p.i.). (**B**) Higher-magnification view of boxed area from **A**. Note strong nuclear and cytoplasmic staining in glial cells (*arrowhead*) and neurons (*arrow*). (**C**) Strong Jab1 staining in endothelial cells lining blood vessel (*arrowhead*) of the control mice brainstem tissue. (**D**) Decreased Jab1 immunoreactivity in the cytoplasm and nucleus of neurons and glial cells in *ts*1-infected brainstem tissue showing spongiform changes (at 30 d.p.i.). (**E**) Higher-magnification view of black boxed area from **D**. Note the absent or weak nuclear and cytoplasmic staining in neurons (*arrow*). (**F**) Decreased Jab1 staining in endothelial cells lining blood vessel (*arrowhead*) of the *ts*1-infected mice brain stem tissue.

To confirm the WB and IHC results for Jab1, HIF-1$\alpha$, and VEGF, we prepared cDNA from whole brains of control and *ts1*-infected mice and performed semi-quantitative reverse transcriptase–polymerase chain reaction (RT-PCR) analysis. As shown in Figure 5A and B, Jab1 and VEGF mRNA levels were significantly decreased in *ts1*-infected brains at 30 d.p.i. ($^{*}p < .05$) compared with control brains, whereas the HIF-1$\alpha$ mRNA level was unchanged in control and *ts1*-infected brains.

*Increased expression of p53 in the ts1-infected brains*

Previous reports showed that Jab1 is involved in p53 cytoplasmic localization and degradation, and that Jab1 knockout mice had higher p53 leves (Oh *et al*, 2006; Tomoda *et al*, 2004). To determine if a decreased level of brain Jab1 protein will lead to an increase in p53 protein, we analyzed the amount of p53 by immunoblotting of brain homogenates of control and *ts1*-infected mice. Figure 6A and B show that *ts1* infection induced a significant increase in p53 levels at both 23 and 30 d.p.i. ($^{*}p < .05$; $^{**}p < .01$). This finding is in agreement with results from Kim *et al* (2002), which indicated that MoMuLV-*ts1* infection increases the expression and accumulation of p53 protein and its dependent genes in astrocytes and brainstem.

*Decreased levels of Jab1, HIF-1α, and VEGF in ts1-infected CVE cells*

We also studied the expression of these proteins in CVE cells because among all cell types in the CNS, endothelial cells are the most conspicuous in virus replication and production, although they are not killed by the infection (Shikova *et al*, 1993). To determine the expression of Jab1, HIF-1$\alpha$, and VEGF proteins in *ts1*-infected CVE cells, we performed WB and RT-PCR analysis using whole-cell extracts of control and *ts1*-infected CVE cells at 24, 48 and 72 h post infection. Figure 7A and B show that the level of Jab1 increases at 24 h post infection and then starts to decrease at 48 and 72 h post infection. The levels of HIF-1$\alpha$ and VEGF also significantly decreased at 48 and

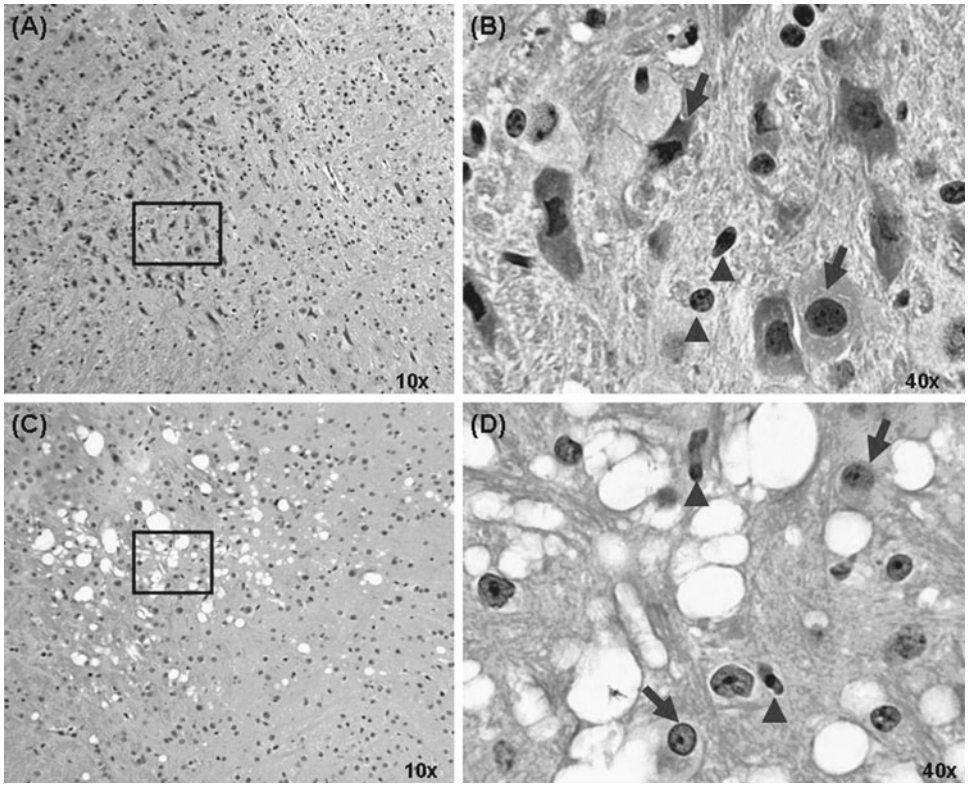


**Figure 3** Expression of HIF-1$\alpha$ in brainstem of control versus *ts*1-infected mice. (**A**) Intense HIF-1$\alpha$ immunoreactivity in the cytoplasm and nucleus of neurons and glial cells in the brainstem of control mice (at 30 d.p.i.). (**B**) Higher-magnification view of black boxed area from **A**. Note strong nuclear and cytoplasmic staining in glial cells (*arrowhead*) and neurons (*arrow*). (**C**) Decreased HIF-1$\alpha$ immunoreactivity in the cytoplasm and nucleus of neurons and glial cells in *ts1*-infected brainstem tissue showing spongiform changes (at 30 d.p.i.). (**D**) Higher-magnification view of black boxed area from **C**. Note the weak or absent nuclear and cytoplasmic staining in glial cells (*arrowhead*) and neurons (*arrow*).

72 h post infection (Figure 7A and B) compared with noninfected cells. The levels of all three proteins, Jab1, HIF-1$\alpha$, and VEGF, were significantly decreased at 72 h post infection compared to noninfected CVE cells. We also determined the levels of Jab1, HIF-1$\alpha$ and VEGF mRNA expression by RT-PCR. Figure 8A and B shows that the levels of Jab1 and VEGF mRNA were increased at 24 h after infections and started to decrease at 48 and 72 h post infection compared to noninfected cells. Compare with Jab1 and VEGF mRNA levels, HIF-1$\alpha$ mRNA level was unchanged in *ts1*-infected CVE cells (Figure 8A).

*Increased expression of p53 in the ts1-infected CVE cells*

The level of p53 protein was analyzed by WB to determine whether p53 protein accumulates in *ts*1-infected CVE cells. We show that p53 protein increased in *ts*1-infected CVE cells at 24, 48, and 72 h post infection compared with controls (Figure 9A and B; * $p < .05$).

## Discussion

The present study shows that MoMuLV-*ts1* infection leads to a decrease in Jab1, HIF-1$\alpha$, and VEGF protein and an increase in p53 protein in *ts1*-infected brains and CVE cells. These results were obtained by WB analysis and confirmed by IHC. Overexpression of p53 is known to lead to cell cycle arrest or apoptosis (Liu *et al*, 1994), and although we have demonstrated an increase expression of p53 in CVE cells, we could not detect cell death even 72 h after *ts1* infection. The result is not surprising to us because it was demonstrated that among all cell types in the CNS, endothelial cells are the most conspicuous in terms of virus replication and production but they are not killed by the infection (Shikova *et al*, 1993). Indeed, it is intriguing that endothelial cells do not show any pathological abnormality upon *ts1* infection. It may be that endothelial cells have the ability to adapt to *ts1* infection by activating their defense system. For example, it was demonstrated that CVE cells promptly respond to the oxidative stress by enhancing expression of several antioxidative enzymes, including superoxide dismutase and glutathione peroxidase (Lu *et al*, 1993). CVE cells may use a similar mechanism of adaptation as astrocytes by mobilizing Nrf2-mediated thiol antioxidant defenses, with up-regulation of plasma membrane cystine/glutamate antiporter (xCT), cystine uptake, and glutathione (GSH) synthesis (Qiang *et al*, 2006).

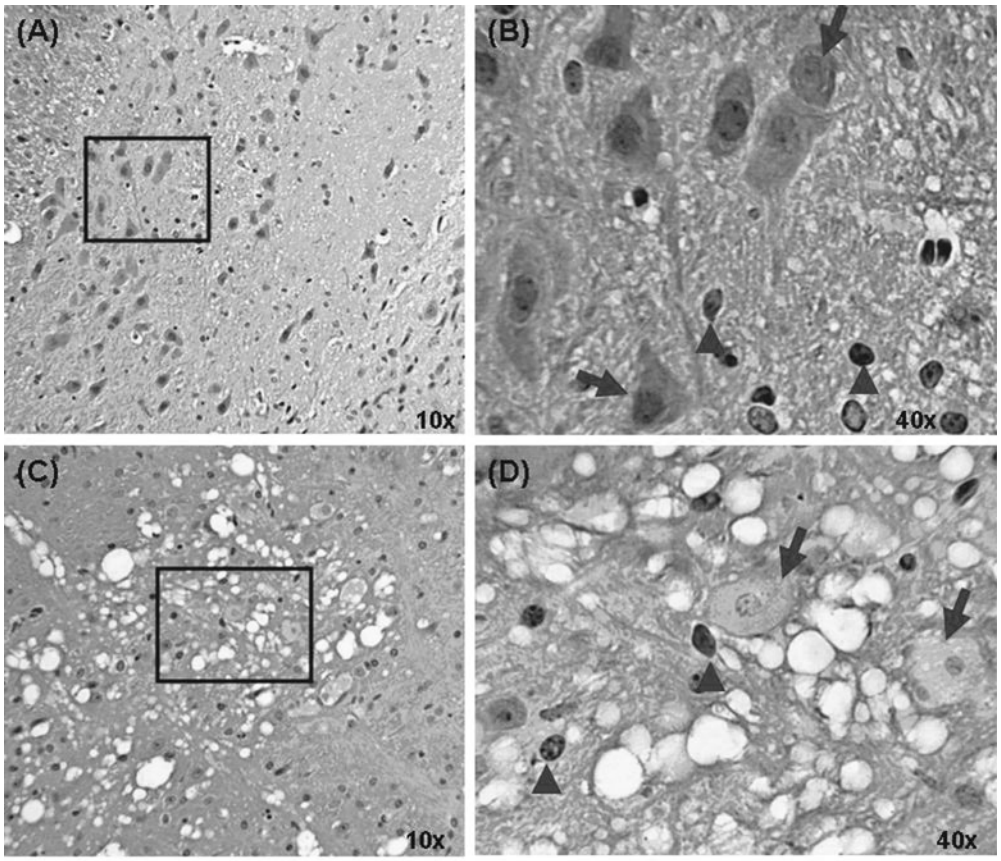


**Figure 4** Expression of VEGF in brainstem of control versus *ts*1-infected mice. (**A**) Intense VEGF immunoreactivity in the cytoplasm and nucleus of neurons and glial cells in the brainstem of control mice (at 30 d.p.i.). (**B**) Higher-magnification view of black boxed area from **A**. Note strong VEGF staining in glial cells (*arrowhead*) and neurons (*arrow*). (**C**) Decreased VEGF immunoreactivity in the cytoplasm and nucleus of neurons in *ts1*-infected brainstem tissue showing spongiform changes (at 30 d.p.i.). (**D**) Higher-magnification view of black boxed area from **C**. Note the weak or absent nuclear and cytoplasmic staining in the neurons (*arrows*). Glial cells nuclei appear labeled (*arrowhead*).

Additionally, we found that *ts1*-infected CVE cells significantly increased the expression and secretion of mature nerve growth factor (NGF), an important factor for cell survival (data not published).

Here we demonstrate that *ts1* infection leads to a decrease in Jab1 protein and mRNA levels in the brain and in CVE cells. The mechanism that leads to this decrease is not yet known and requires further *in vitro* and *in vivo* investigation. However, virus infection can affect cell division by interfering with cell cycle regulation or altering cellular gene expression. Thus, Jab1 protein expression might be altered due to viral infection. This may trigger a variety of events. Overexpression of p53 is a constant feature of viral infection in the central nervous system (Genini *et al*, 2001; Ehsan *et al*, 2000; Kim *et. al*, 2002). We show that *ts1* infection leads to an increase in p53 expression in the brain and in CVE cells. We speculate that a reduction in Jab1 protein levels would lead to further accumulation of p53 in the cells because previous studies showed that Jab1 is involved in p53 localization, subsequently leading to the degradation of p53 (Oh *et al*, 2006), and suggesting that the maintenance of p53 homeostasis requires the presence of Jab1. Regulation of p53 protein levels is achieved primarily via posttranslational mechanisms, although there might be other signals responsible for regulation of p53 besides Jab1.

According to the previous studies, hypoxia is a physiologic inducer of p53 (Blagosklonny *et al*, 1997). HIF-1$\alpha$ can undergo protein-protein interaction with either Jab1 or p53 during hypoxia and Jab1 and p53 compete for binding, because Jab1 and p53 interact with the same domain on HIF-1$\alpha$ (Bae *et al*, 2002). Binding of p53 to HIF-1$\alpha$ results in HIF-1$\alpha$ degradation facilitated by a HIF-1$\alpha$ ubiquitination by the Hdm2-complexes, whereas binding of Jab1 stabilizes HIF-1$\alpha$ and increases the capacity of HIF-1$\alpha$ to act as a transactivator (Bae *et al*, 2002). Although some reports demonstrated that association of HIF-1$\alpha$ and p53 results in inhibition of HIF-stimulated transcription, other studies showed that p53 not only promotes the proteasomal degradation of the $\alpha$ subunit of HIF-1 but also inhibits angiogenesis by down-regulating VEGF (Ravi *et al*, 2000; Blagosklonny *et al*, 1997). Another report (Pal *et al*, 2001) showed

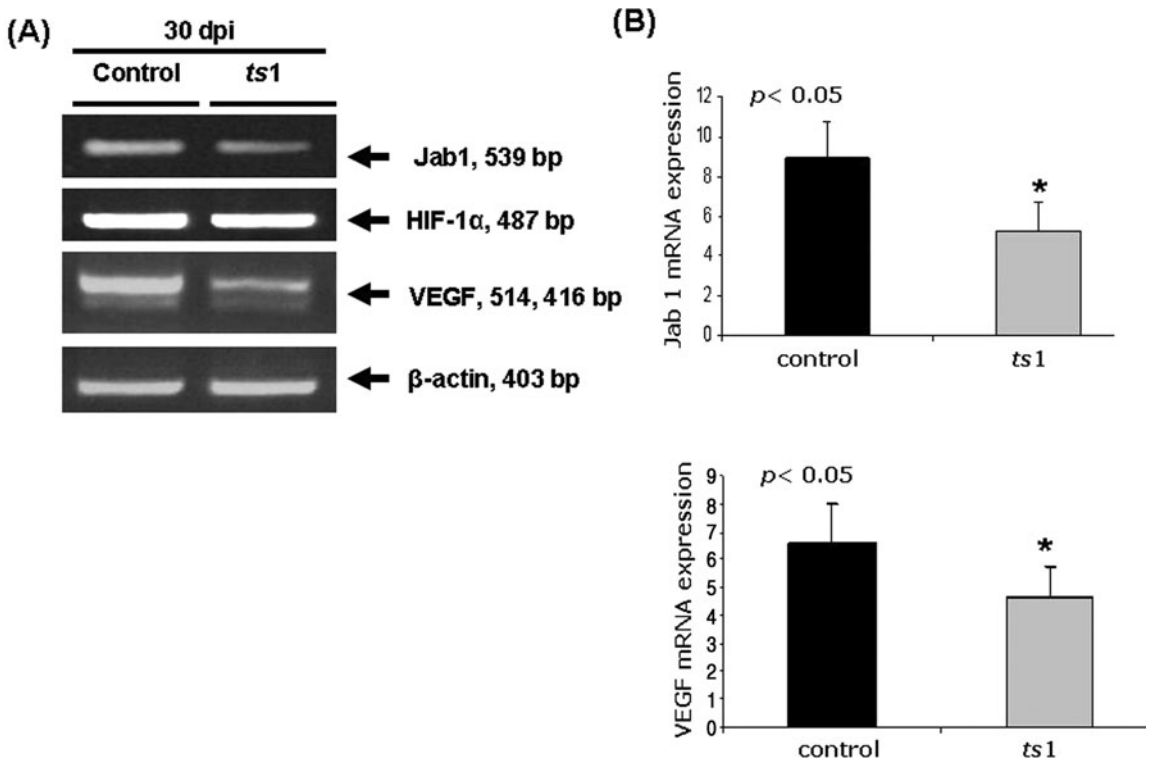


**Figure 5** Decreased expression of Jab1 and VEGF mRNA in the *ts*1-infected mice brains. (**A**) Semi-quantitative RT-PCR analyses for Jab1, HIF-1$\alpha$, and VEGF mRNAs from whole brains of control and *ts*1-infected mice sacrificed at 30 d.p.i. Notice the decreased levels of Jab1 and VEGF mRNAs in *ts1*-infected brains compared with uninfected brains. For VEGF two alternative splicing variants were identified. A 514-bp product, corresponding to the VEGF188, and a second 462-bp product, corresponding to the VEGF164 isoform, were detected. VEGF188 isoform expression was greater than of VEGF 164. The HIF-1$\alpha$ mRNA levels were unchanged in control and *ts1*-infected brains. (**B**) Densitometric analysis of Jab1 and VEGF mRNA levels in the brain of *ts*1-infected versus control mice. Amounts of Jab1 and VEGF mRNAs in brain of *ts*1-infected mice were significantly decreased (* $p < .05$), compared to those of the brains of control mice. The results represent the mean $\pm$ standard deviation for three independent experiments.

that, like normoxic conditions, p53 down-regulates the hypoxic induction of VEGF transcription by preventing the binding of Sp1 to its promoter. The authors concluded that like HIF-1$\alpha$, Sp1 also plays a significant role in promoting VEGF transcription in breast cancer cells under hypoxic conditions.

We found that *ts1* infection leads to a reduction of HIF-1$\alpha$ protein levels, but not mRNA expression in the infected brain and CVE cells, which probably is due to accumulation of p53 in *ts1*-infected CNS and binding to HIF-1$\alpha$ in favor of Jab1. A post-translational alteration of HIF-1$\alpha$ protein levels may account for unaltered HIF-1$\alpha$ mRNA levels in *ts*1-infected samples compared with controls. Therefore, the ratio of Jab1:p53 is likely to play a crucial role in determining the direction of the cellular response to acute hypoxia and cellular stress (Ravi *et al.*, 2000; Blagosklonny *et al*, 1998; Hansson *et al*, 2002). Our IHC analysis showed a weak staining of HIF-1$\alpha$ in the cytoplasm and a weak or absent staining for HIF-1$\alpha$ in the nucleus in *ts1*-infected brainstems compared with control brain where HIF-1$\alpha$ showed intense labeling in both compartments. This suggests that HIF-1$\alpha$ is rapidly degraded in the cytoplasm due to *ts1* infection. Very interesting is the fact that a previous study (Goda *et al*, 2003) demonstrated that loss of HIF-1$\alpha$ abolished hypoxia-induced growth arrest in a p53-independent fashion. It was demonstrated that loss of HIF-1$\alpha$ in B cells results in progression into S phase during hypoxia and, along with other findings, that p53 did not contribute directly to hypoxia-induced growth arrest (Goda *et al*, 2003). This is particularly relevant for our study because we showed that the level of p53 is elevated and that level of HIF-1$\alpha$ is down-regulated in endothelial cells without any significant cell loss.

VEGF, in general, is neuroprotective and significantly contributes to neuronal protection under hypoxic conditions. Decreases in VEGF production could therefore be detrimental to neurons. A faster degradation of HIF-1$\alpha$ would lead to a decrease in VEGF expression in the infected brain and a loss of neuroprotection. We found that VEGF protein and mRNA levels were reduced in *ts*1-infected brains and *ts*1-infected CVE cells. IHC showed a dramatic decrease in levels of VEGF in the neurons of *ts*1-infected brainstem compared with control brainstems. Further investigation will be necessary to determine if VEGF levels were also decreased in the *ts*1-infected glial cells, such as astroctytes and microglial. The

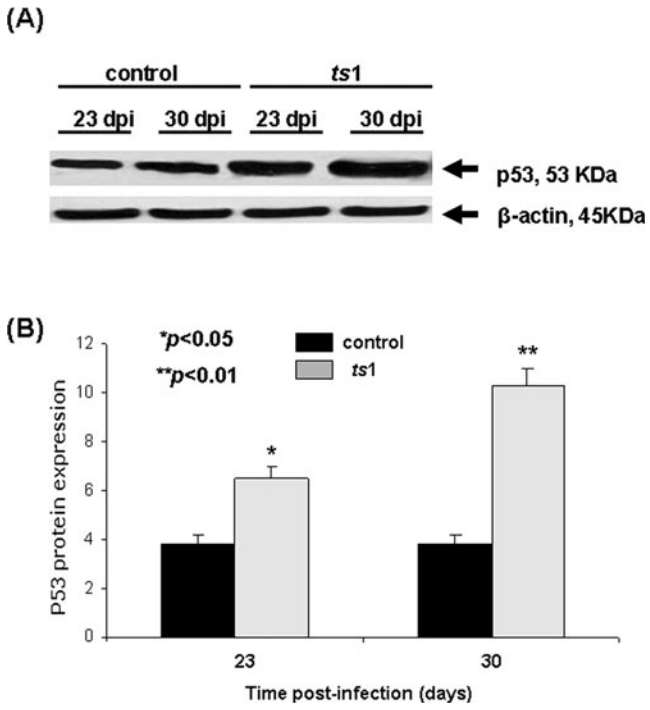


**Figure 6** Increased expression of p53 in brains of *ts*1-infected mice. (**A**) Western blots showing increased levels of p53 proteins in whole brain of controls versus *ts*1-infected mice at 23 and 30 d.p.i. $\beta$-Actin served as a loading control. (**B**) Densitometric analysis of p53 protein levels in the whole brain of *ts*1-infected versus control mice. Levels of p53 proteins were significantly increased in *ts*1-infected brain at 23 ($^*p < .05$) and 30 ($^{**}p < .01$) d.p.i. compared to those of the brains of control mice. The results represent the mean $\pm$ standard deviation for three independent experiments.

exact mechanism of decreased VEGF levels in *ts1* infection is not known and needs to be further investigated, both *in vitro* and*in vivo.* This finding does not mean that a reduction in HIF-1$\alpha$ is the only factor involved in VEGF reduction.

A proposed sequence of events from a decrease in Jab1 protein expression to a decrease in VEGF production and release from CVE cells in *ts*1-infected brains is described in Figure 10. The data presented here support the idea that *ts1*-mediated neurodegeneration it might be caused by a reduction in VEGF level from endothelial cells or other cells, resulting from a decrease in Jab1 protein. Elucidation of the mechanism (s) for decreased Jab1 expression will require further analysis, both *in vivo* and *in vitro.*

## Materials and methods

*Reagents*
Sodium orthovanadate ($Na_3VO_4$), sodium $\beta$-glycerophosphate, sodium fluoride (NaF), and phenylmethylsulfonyl fluoride were purchased from Sigma-Aldrich Chemical Company (St. Louis, MO, USA). Leupeptin, pepstatin, and aprotinin were purchased from Boehringer Mannheim (Indianapolis, IN, USA). Iscove's modified Dulbecco's medium (IMDM) was purchased from Invitrogen (Carlsbad, CA, USA).

*Virus*
*ts1*, a spontaneous temperature-sensitive mutant of MoMuLV, was propagated in TB cells, a thymus-bone marrow cell line. Virus titers were determined using a modified direct focus assay in the 15F cell line, a murine sarcoma-positive, leukemia-negative cell line, as described previously (Wong *et al*, 1981).

*Animals and virus inoculation*
Animals used for these experiments, FVB/N, were obtained from Taconic Farms (Germantown, NY, USA). Newborn FVB/N mice were inoculated intraperitoneally with 0.1 ml of *ts1* viral suspension containing $10^6$ to $10^7$ infection units/ml, as previously described (Kim *et al*, 2002). Control mice were inoculated with medium only. The mice were observed daily for clinical signs of disease and euthanized at 23 and 30 d.p.i. The experimental protocol was approved by the Texas A&M University Institutional Animal Care and Use Committee.

*Cell culture and virus infection*
CVE cells were obtained from the brain of 2- to 4-week-old BALB/c mice and were kindly provided to us by Dr. Jane Welsh, Texas A&M University (Tennakoon *et al*, 2001). The cells were maintained IMDM supplemented with 10% fetal bovine serum (Invitrogen) and antibiotics (100 units/ml penicillin and 100 $\mu$g/ml streptomycin). Cells were grown at 37$^o$C in a humidified incubator containing 5% $CO_2$. For virus infection, CVE cells ($4 \times 10^5$) in IMDM containing 2% fetal bovine serum (FBS) and 4 $\mu$g/ml polybrene were seeded in 100-mm tissues culture dishes. After culturing overnight, the medium was removed and the cells were infected with *ts1* virus at a multiplicity of infection of 10 in IMDM containing 2% FBS and 4 $\mu$g/ml polybrene and incubated for 1 h at 37$^o$C under 5% $CO_2$. After virus absorption, the medium containing the virus was removed and IMDM containing 10% FBS added to the culture. The plates were then incubated for various times. As a control, CVE cells were treated identically, except that the medium used was IMDM containing polybrene only.

*Tissue processing*
For histopathology and immunohistochemistry (IHC), *ts*1-infected ($n = 3$) and control ($n = 3$) mice were euthanized with using an intraperitoneal injection of pentobarbital (150 mg/kg) and perfused with 10% buffered formalin, using a peristaltic pump. For RT-PCR and Western blotting (WB) analyses of mRNAs and proteins, respectively, control ($n = 3$) and *ts*1-infected ($n = 3$) mice were sacrificed, their whole brain removed, snap-frozen in liquid nitrogen, and stored at $-80^\circ$C.

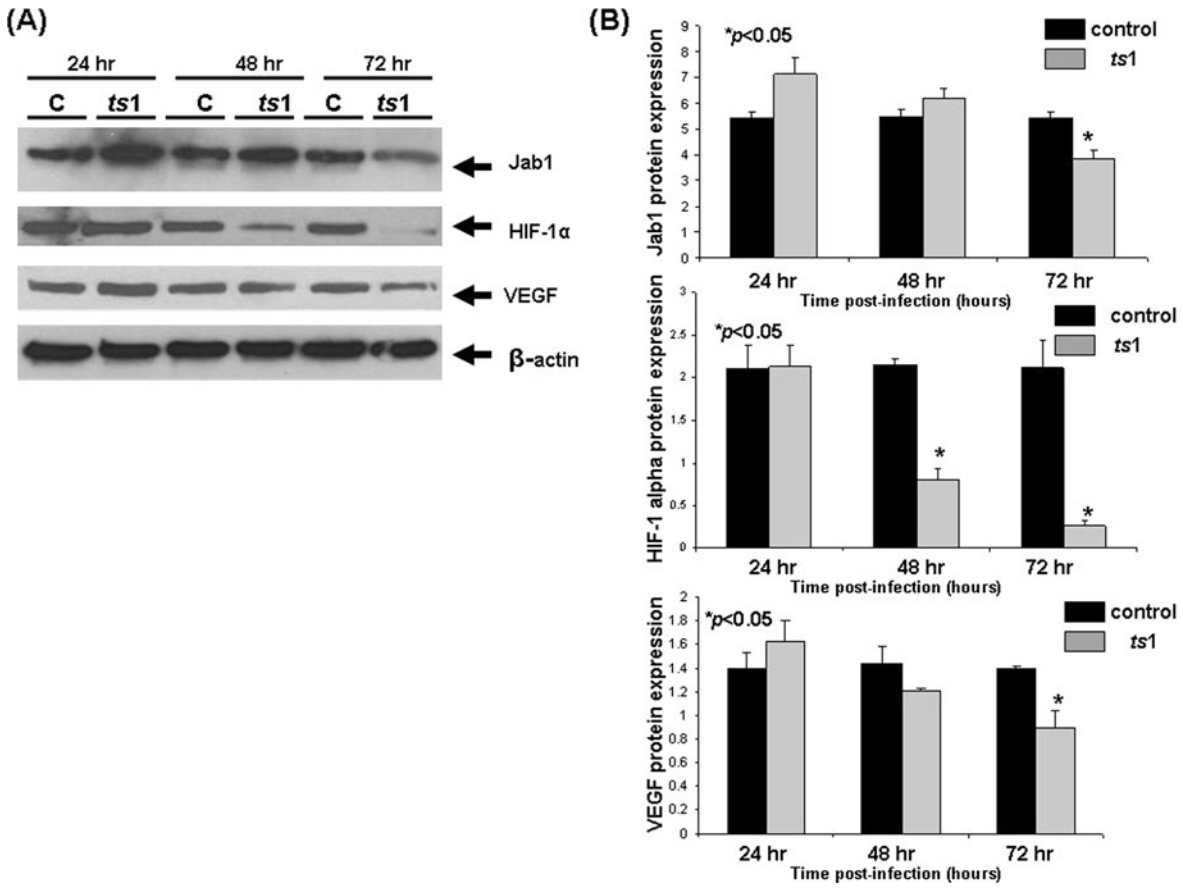


**Figure 7** Expression of Jab1, HIF-1$\alpha$, and VEGF proteins in controls and *ts*1-infected CVE cells. (**A**) Western blots showing levels of Jab1, HIF-1$\alpha$, and VEGF proteins in *ts*1-infected CVE cells at 24, 48, and 72 h post infection compared with uninfected cells. (**B**) Densitometric analysis of Jab1, HIF-1$\alpha$, and VEGF protein levels in *ts1*-infected CVE cells. Jab1 protein expression increases at 24 h and decreases at 48 h and significantly decreases at 72 h post infection (* $p < .05$) compared with uninfected cells. Levels of HIF-1$\alpha$ proteins significantly decreases at 48 (* $p < .05$) and 72 (* $p < .05$) h post infections but were unchanged at 24 h post infection compared with untreated cells. VEGF expression levels increases at 24 h post infection and significantly decreases at 48 and 72 h post infection (* $p < .05$). $\beta$-Actin served as a loading control. The results represent the mean $\pm$ standard deviation for three independent experiments.

*Tissue and cell extracts*

For WB analysis, tissues lysates were prepared by homogenization of frozen tissues (whole brain) in 15 volumes of lysis buffer containing 50 mM Tris-HCl (pH 7.4), 150 mM NaCl, 1 mM $CaCl_2$, 1 mM $MgCl_2$, 0.1% Triton X-100, 50 mM NaF, 10 mM phenylmethylsulfonyl fluoride, 10 $\mu$g/ml papstatin, 10 $\mu$g/ml leupeptin, and 5 $\mu$g/ml aprotinin. The lysates were cleared by centrifugation at 13,000 $\times$ *g* at 4°C for 30 min and the supernatant kept frozen at −80°C. The CVE cells were washed twice with cold Hanks' balanced salt solution and lysed in lysis buffer. The lysates were cleared by centrifugation at 13,000 $\times$ *g* at 4°C for 30 min and the supernatant kept frozen at −80°C. The protein content of the lysates was determined using the Bradford Assay (Bio-Rad Laboratories, Hercules, CA), with bovine serum albumin as the standard.

*Immunohistochemistry*

Because we determined previously that histologically detectable neuronal loss is evident at 25 to 30 d.p.i. (Choe *et al*, 1998), we performed all of the immunohistochemical analyses using brains from *ts1*-infected mice and age-matched noninfected control mice at 30 d.p.i. Five-micron paraffin-embedded sections were used for immunohistochemical study. After deparafinization, the sections were subjected to an antigen retrieval protocol by heating them in 10 mM citrate buffer (pH 6.0) for 10 min. Potential nonspecific binding sites were blocked with 5% normal goat or rabbit serum in phosphate-buffered saline. After blocking, the sections were incubated for 1 h to overnight with primary antibody. Primary antibodies, specific for Jab1, HIF-1$\alpha$, and VEGF-A, were purchased from Santa Cruz Bitotechology (Santa Cruz, CA, USA) and a 1:50 dilution was used. Following primary antibody reaction, sections were washed and incubated with either biotin-conjugated anti-rabbit or anti-mouse immunoglobulin G (IgG) (Vector Laboratories, Burlingame, CA, USA). A Vector-ABC streptavidin-peroxidase kit (KPL, Maryland, USA) with a benzidine substrate for color was used for color development. Counterstaining was done with diluted

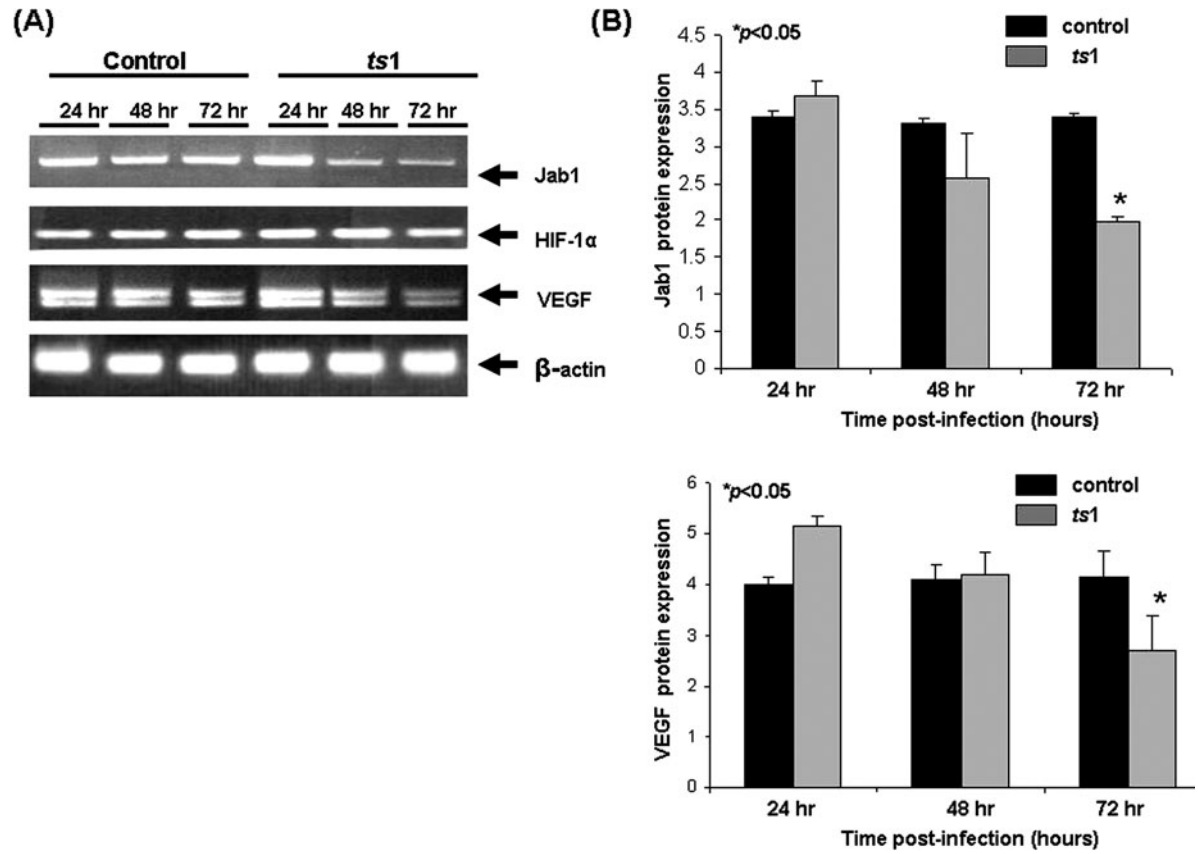


**Figure 8** Expression of Jab1, HIF-1$\alpha$, and VEGF mRNA in *ts*1-infected CVE cells. (**A**) RT-PCR showing levels of Jab1, HIF-1$\alpha$, and VEGF mRNA in *ts*1-infected CVE cells at 24, 48, and 72 h post infection compared with uninfected cells. (**B**) Densitometric analysis of Jab1, HIF-1$\alpha$, and VEGF mRNA levels in *ts1*-infected CVE cells. Jab1 mRNA expression increases at 24 h and decreases at 48 and 72 h post infection (* $p < .05$). The levels of HIF-1$\alpha$ mRNA were unchanged in *ts1*-infected versus control CVE cells. The levels of VEGF mRNA decreases at 48 and 72 h post infection (* $p < .05$) after an increase at 24 h post infection. $\beta$-Actin served as a loading control. The results represent the mean $\pm$ standard deviation for three independent experiments.

hematoxylin. Sections that were not incubated with primary antibody served as negative controls.

*Western blot analysis*

Proteins (15 to 30 $\mu$g) were separated by electrophoresis and transferred to nitrocellulose membranes (Schleicher and Schuell, Keene, NH, USA). Membranes were incubated for 1 h in blocking buffer (20 mM Tris-HCl–buffered saline containing 5% nonfat milk powder and 0.1% Tween 20) at room temperature, then probed with appropriate antibodies in blocking buffer or blocking buffer including 5% bovine serum albumin instead of 5% nonfat milk overnight at 4°C. Blots were incubated at 4°C overnight with anti-Jab1 (1:200), anti-p53 (1:200), anti-HIF-1$\alpha$ (1:200), or anti-VEGF-A, (1:200) antibodies (all antibodies from Santa Cruz Biotechnology). Monoclonal mouse IgG antibody against $\beta$-actin was purchased from Sigma-Aldrich Chemical (St. Louis, MO, USA). The blots were washed extensively, and then incubated for 1 h with a 1:5000 or 1:10000 dilution of secondary antibody. Peroxidase labeled anti-rabbit (1:10000) and anti-mouse secondary antibody (1:5000) were purchased from Kirkegaard and Perry Laboratories (Gaithersburg, MD, USA). After additional washes, the blots were incubated with Super Signal West Pico chemiluminescent substrate according to directions in the kit (Pierce, Rockford, IL, USA).

*Total RNA extraction and semi-quantitative RT-PCR*

Total RNA was extracted from whole-brain tissues and CVE cells using an SV RNA extraction kit (Promega, Madison, WI, USA), according to manufacturer's directions. RNA was quantified by absorbance at 260 nm. Using a Super Script III First Strand Synthesis System (Invitrogen), 100 ng of total RNA was amplified by reverse transcriptase–polymerase chain reaction (RT-PCR) and the cDNAs were amplified.

- Jab1 primers: forward, 5′-GTGATGGGTCTGATGCT AGGAA -3′; reverse, 5′-AGCAAGCTAGAAGAA CTCAACG-3′ (Korbonits *et al*, 2002)
- HIF-1$\alpha$ primers: forward, 5′-GTCGGACAGCCTCA CCAAACAGAGC-3′; reverse, 5′-GTTAACTTGAT CCAAAGCTCTGAG-3′; (Turcotte *et al*, 2003)
- VEGF primers: forward, 5′-GACCCTGGTGGACAT CTTCCAGGA-3′; reverse, 5′-GGTGAGAGGTCTAG TTCCCGA-3′; (Wang and Keiser, 1998)

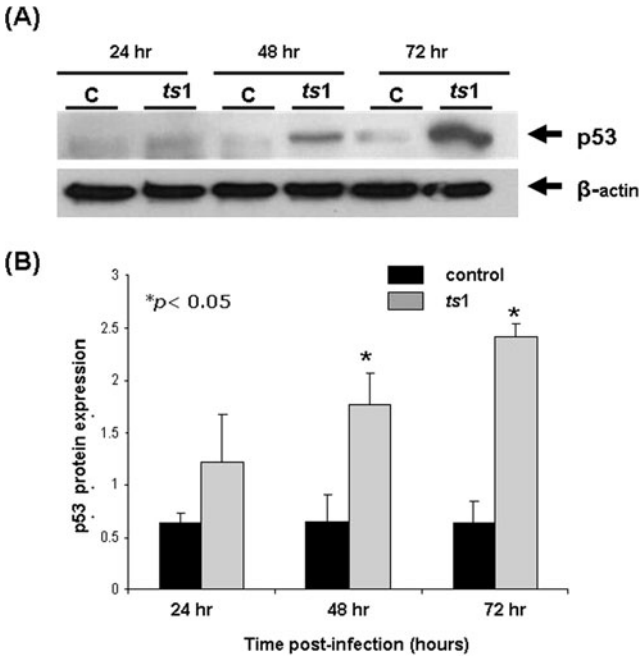


**Figure 9** Increased expression of p53 protein in *ts*1-infected CVE cells. (**A**) Western blots showing increased levels of p53 proteins in *ts*1-infected CVE cells at 24, 48 and 72 h post infection compared with uninfected cells. $\beta$-Actin served as a loading control. (**B**) Densitometric analysis showing increase in p53 levels in *ts1*-infected cells at 24, 48 (* $p < .05$), and 72 (* $p < .05$) h post infection. The results represent the mean $\pm$ standard deviation for three independent experiments.

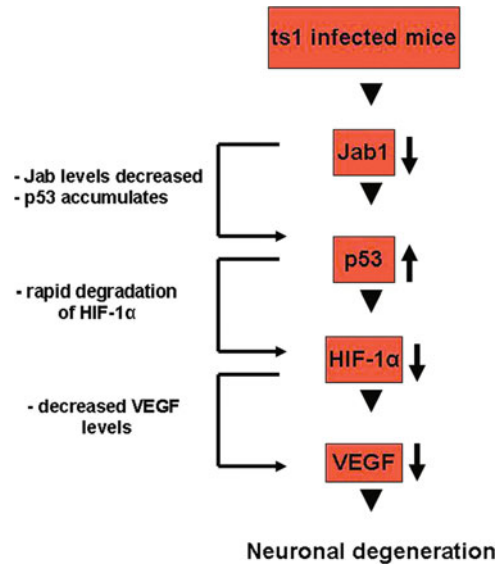


**Figure 10** Proposed mechanism which might lead to reduced VEGF levels and neuroprotection in *ts1* infection. *ts*1 infection can lead to decrease Jab1 levels which in turn affects p53 protein levels. The p53 protein accumulates and may be responsible for a rapid degradation of HIF-1$\alpha$ and reduced VEGF levels. A reduction of VEGF levels plays an important role in neurodegeneration in *ts*1-infected mice.

- $\beta$−Actin primers: forward, 5′- ATGTACGTAAGCC AGGC-3′; reverse, 5′-AAGGAACTGGAAAAGAGC -3′ (Mendes *et al*, 2006)

Expected size for the Jab1 PCR product was 539 base pairs (bp). For Jab1, 26 cycles were carried out with 1 min at 91°C, 1 min at 58°C, and 1 min at 72°C, after a denaturing cycle of 95°C, 15 s. Expected size for the HIF-1$\alpha$ PCR product was 487 (bp). For HIF-1$\alpha$, 25 cycles were carried out with 30 s at 95°C, 1 min at 55°C, and 2.5 min at 72°C. A final extension of 7 min at 72°C was carried out. For VEGF, one set of rat primers, which amplified two splice variants of a rat VEGF mRNA ($VEGF_{164}$ and $VEGF_{188}$) was used. The PCR profile consisted of initial denaturation at 94°C for 7 min, followed by 35 cycles of denaturation at 94°C for 30 s, annealing at 58°C for 30 s, extension at 72°C for 90 s, and extension at 72°C for 7 min. The expected length of the PCR products was 462 bp for $VEGF_{164}$, and 514 bp for $VEGF_{188}$. To demonstrate the integrity of the RNA samples used in the RT-PCR reactions, parallel amplifications with oligonucleotide primers for mouse $\beta$-actin were performed. The expected size for the $\beta$-actin PCR product was 403 bp. PCR fragments were analyzed on 1.5% agarose gels stained with ethidium bromide.

*Statistical analysis*

Quantification of the WB and semiquantitation of RT-PCR band density was performed on a Macintosh computer using the public domain NIH Image program (developed at the U.S. National Institutes of Health and available on the Internet at http://rsb.info.nih.gov/nih-image. Data were presented as mean $\pm$ SD, and statistical comparisons were made using Student $t$ test. A $p$ value of $<.05$ was considered statistically significant. Data are representative of three independent experiments.

## References

Bae MK, Ahn MY, Jeong JW (2002). Jab1 interacts directly with HIF-1$\alpha$ and regulates its stability. *J Biol Chem* **277:** 9–12.

Bench-Otschir D, Kraft R, Huang X, Henklein P, Kapelari B (2001). COP9 signalosome-specific phosphorylation targets p53 to degradation by the ubiquitin system. *EMBO J* **20:** 1630–1639.

Blagosklonny MV, An GW, Ramanova LY, Trepel J, Fojo T, Neckers L (1998). p53 inhibits hypoxia-inducible factor-stimulated transcription. *J Biol Chem* **273:** 11995–11998.

Choe W, Stoica G, Lynn W, Wong PKY (1998). Neurodegeneration induced by MoMuLV-ts1 and increased expression of Fas and TNF-$\alpha$ in the central nervous system. *Brain Res* **779:** 1–8.

Clark S, Duggan J, Chakraborty J (2001). Ts1 and LP-BM5: a comparison of two murine retrovirus models for HIV. *Viral Immunol* **14:** 95–109.

Genini D, Sheeter D, Rought S, Zaunders JJ, Susin SA, Kroemer G, Richman DD, Carson DA, Corbeil J, Leoni LM (2001). HIV induces lymphocyte apoptosis by a p53-initiated, mitochondrial-mediated mechanism. *FASEB J* **15:** 5–6.

Goda N, Ryan HE, Khadivi B, McNulty W, Ricket RC, Johnson RS (2003). Hypoxia-inducible factor 1 alpha is essential for cell cycle arrest during hypoxia. *Mol Cell Biol* **23:** 359–369.

Ehsan A, Fan H, Eagan PA, Siddiqui HA, Gulley ML (2000). Accumulation of p53 in infectious mononucleosis tissues. *Hum Pathol* **31:** 1397–1403.

Hansson LO, Friedler A, Freud S, Rudiger S, Fersht AR (2002). Two sequence motifs from HIF-1$\alpha$ bind to the DNA-binding site of p53. *Proc Natl Acad Sci U S A* **99:** 10305–10309.

Kim HT, Tasca S, Qiang W, Wong PKY, Stoica G (2002). Induction of p53 accumulation by moloney murine leukemia viru-*ts1* infection in astrocyets via activation of extracellular signal-regulated kinases 1/2. *Lab Invest* **82:** 693.

Korbonits M, Chahal HS, Kaltsas G, Jordan S, Urmanova Y, Khalimova Z, Harris PE, Farrell EW, Claret FX, Grossman AB (2002). Expression of phosphorylated p27Kip1 protein and jun activation domain-binding protein 1 in human pituitary tumors. *J Clin Endocrinol Metab* **87:** 2635–2643.

Lee E, Oh W, Song J (2006). Jab1 as a mediator of nuclear export and cytoplasmic degradation of p53. *Mol Cells* **22:** 133–140.

Liu M, Dhanwada KR, Birt DF, Hecht S, Pelling JS (1994). Increase p53 protein half-life in keratinocytes followinf UV-B radiation. *Carcinogenesis* **15:** 1089–1092.

Lu D, Maulik N, Moraru II, Kreutzer DL, Das DK (1993). Molecular adaptation of vascular endothelial cells to oxidative stress. *Am J Physiol* **264:** 715–722.

Mendes O, Kim HT, Stoica G (2005). Expression of MMP-2, MMP-9 and MMP-3 in breast cancer brain metastasis in a rat model. *Clin Exp Metastasis* **22:** 237–246.

Oh W, Lee EW, Sung YH, Yang MR, Ghim J (2006). Jab1 induces the cytoplasmic localization and degradation of p53 in coordination with Hdm2. *J Biol Chem* **281:** 17457–17465.

Oono K., Yoneda T, Manabe T, Yamagishi S, Matsuda S, Hitomi J, Miyata S, Mizuno T, Imaizumi K, Katayama T, Tohyama M (2004). JAB1 participates in unfolded preotein responses by association and dissociation with IRE1. *Neurochem Int* **45:** 765–772.

Oosthuyse B, Moons L, Storkebaum E, Beck H, Nuyens D (2001). Deletion of hypoxia-response element in the vascular endothelial growth factor promoter causes motor neuron degeneration. *Nat Genet* **28:** 131–138.

Pal S, Datta K, Mukhopadhyay D (2001). Central role of p53 in regulation of vascular permeability factor/ vascular endothelial growth factor (VPF/VEGF) expression in mammary carcinoma. *Cancer Res* **61:** 6952–6957

Prasad G, Stoica G, Wong PKY (1989). The role of thymus in the pathogenesis of hind-limb paralysis induced by ts1, a mutant of Moloney murine leukemia virus-TB. *Virology* **169:** 332–340.

QiangW, Kuang X, Liu J, Liu N, Scofield VL, Reid AJ, Jiang Y, Stoica G, Lynn WS, Wong PKY (2006). Astrocytes survive chronic infection and cytopathic effects of the *ts*1 mutant of the retrovirus moloney murine leukemia virus by upregulation of antioxidant defenses. *J Virol* **80:** 3273–3284.

Ravi R, Mookerjee B, Bhujwala ZM, Sutter CH, Artemov D, Zeng Q, Dillehay LE, Madan A, Semeza GL, Bedi A (2000). Regulation of tumor angiogenesis by p53-induced degradation of hypoxia-inducible factor 1$\alpha$. *Genes Dev* **14:** 34–44.

Rempe DA, Lelli KM, Vangeison G, Johnson SR, Federoff KJ (2007). In cultured astrocytes, p53 and MDM2 do not alter hypoxia-inducible factor 1-$\alpha$ function regardless of the presence of DNA damage. *J Biol Chem* **282:** 16187–201.

Shikova E, Lin YC, Saha K, Brooks R, Wong PKY (1993). Correlation of specific virus-astrocyte interactions and cytophatic effects induced by *ts1*, a neurovirulent mutant of Moloney murine leukemia virus. *J Virol* **67:** 1137–1147.

Stoica G, Illanes O, Tasca SI, Wong PKY (1993). Temporal central and peripheral nervous system changes induced by a paralytogenic mutant of Moloney murine leukemia virus TB. *Lab Invest* **69:** 724–735.

Stoica G, Tasca SI, Wong PKY (2000). Motor neuronal loss and neurofilament-ubiquitin alteration in MoMuLV-ts1 encephalopathy. *Acta Neuropathol (Berl)* **99:** 238–244.

Storkebaum E, Lambrechts D, Carmeliet P (2004). VEGF: once regarded as a specific angiogenic factor, now implicated in neuroprotection. *Bio Essays* **26:** 943–954.

Szurek PF, Yuen PH, Ball JK, Wong PK (1990). A Val-25-to-Ile substitution in the envelope precursor polyprotein, gPr80env, is responsible for the temperature sensitivity, inefficient processing of gPr80env, and neurovirulence of ts1, a mutant of Moloney murine leukemia virus TB. *J Virol* **64:** 467–475.

Tennakoon DK, Smith R, Steward MD, Spencer TE, Nayak M, Welsh CJR, (2001). Ovine IFN-$\tau$ modulates the expression of MHC antigens on murine cerebrovascular endothelial cells and inhibits replication of Theiler's virus. *J Interferon Cytokine Res* **21:** 785–792.

Tomoda K, Yoneda-Kato N, Fukumoto A, Yamanaka S, Kato JY (2004). Multiple functions of Jab1 are required for early embryonic development and growth potential in mice. *J Biol Chem* **279:** 43013–43018.

Turcotte S, Desrosiers RR, Beliveau R (2003). HIF-1$\alpha$ mRNA and protein upregulation involves Rho GTPase expression during hypoxia in renal cell carcinoma. *J Cell Sci* **15.**

Wang H, Keiser JA (1998). Vascular endothelial growth factor upregulates the expression of matrix metalloproteinases in vascular smooth muscle cells: role of flt-1. *Circ Res* **83:** 832–840.

Wong PKY, Floyd E, Szurek PF (1991). High susceptibility of FVB/N mice to the paralytic disease induced by *ts*1, a mutant of Moloney murine leukemia virus TB. *Virology* **180:** 365–371.

Wong PKY, Knupp C, Yuen PH, Soong MM, Zachary JF, Tompkins WAF (1985). *ts1*, a paralytogenic mutant of Moloney murine leukemia virus TB, has an enhanced ability to replicate in the central nervous system and primary nerve cell culture. *J Virol* **55:** 60–767.

Wong PKY, Prasad G, Hansen J, Yuen PH (1989). *ts*1, a mutant of Moloney murine leukemia virus-TB, causes both immunodeficiency and neurologic disorders in BALB/c mice. *Virology* **170:** 450–459.

Wong PKY, Soong MM, Yuen PH (1981). Replication of leukemia virus in heterologous cells: Interaction between ecotropic and xenotropic viruses. *Virology* **109:** 366–378.

Yuen PH, Szurek PF (1989). The reduced virulence of the thymotropic Moloney murine leukemia virus derivative MoMuLV-TB is mapped to 11 mutations within the U3 region of the long terminal repeat. *J Virol* **63:** 471–480.